Journal of Colloid and Interface Science 454 (2015) 80–88

Contents lists available at ScienceDirect

Journal of Colloid and Interface Science

www.elsevier.com/locate/jcis

Engineering filamentous bacteriophages for enhanced gold binding and metallization properties

Nuriye Korkmaz Zirpel *, Taner Arslan, Hyeji Lee

Korea Institute of Science and Technology, Europe Forschungsgesellschaft mbH, Campus E 71, Saarbruecken D-66123, Germany

GRAPHICAL ABSTRACT

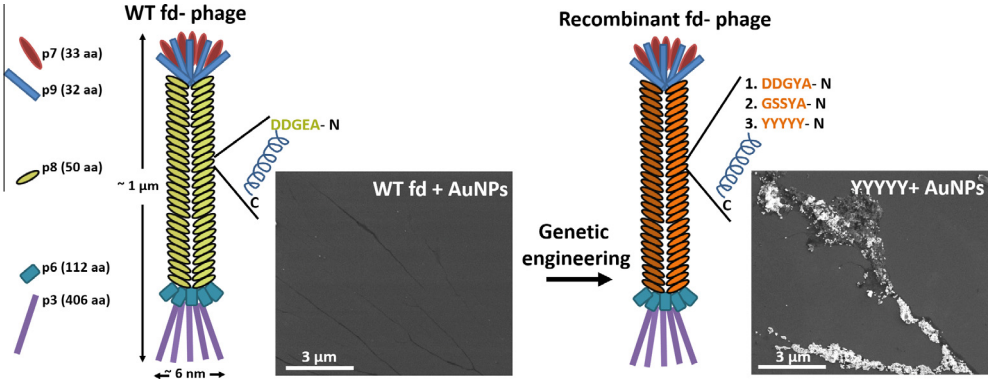

ARTICLE INFO

Article history:
Received 12 March 2015
Accepted 5 May 2015
Available online 13 May 2015

Keywords:
Bottom-up manufacturing
Self-assembly
Bacteriophage
Genetic engineering
Nanoparticle

ABSTRACT

Filamentous bacteriophages are nanowire-like virion molecules consisting of a single stranded DNA (ssDNA) as the genomic material packed in a protein cage. In this study, Tyr containing 5-mer peptides were displayed on phage filaments for enhanced Au binding and reduction properties. Wild type fd (AEGDD) and engineered YYYYY, AYSSG and AYGDD phages were investigated by Quartz crystal microbalance (QCM), Atomic force microscopy (AFM), Scanning electron microscopy (SEM) and Energy dispersive X-ray spectroscopy (EDX) analyses. Presence of only one Tyr unit on five aa flexible region of p8 coat proteins increased Au binding affinities of engineered phages. YYYYY phages were shown to have the strongest Au surface and AuNP binding affinities. Recombinant phages were shown to be coated with Au clusters after one-step metallization reaction. With further genetic modifications, phages can be programmed to function as site specific self-assembling biotemplates for bottom-up manufacturing in nanoelectronics and biosensor application studies.

1. Introduction

Bacteriophages are virus particles infecting only bacteria. F-specific filamentous (Ff) group bacteriophages include M13, fd and f1 phages with almost identical structures [1]. They amplify themselves in Gram negative bacteria carrying F-pili [2]. Wild type (WT) fd phages (~7 nm × 880 nm) are composed of a single stranded DNA (6408 bases) packed in a protein cage of coat proteins. The ssDNA is surrounded by 2750 copies of major coat protein p8 α-helical subunits composed of 50 amino acid (aa) residues. On head and tail parts of the phage, five copies of minor coat proteins p7, p9 and p3, p6 are found

* Corresponding author. Fax: +49 681 9382 240.
E-mail addresses: n.korkmaz@kist-europe.de (N. Korkmaz Zirpel), t.arslan@kist-europe.de (T. Arslan), cccoonu@naver.com (H. Lee).

http://dx.doi.org/10.1016/j.jcis.2015.05.006
0021-9797/

respectively [3–5]. Bacteriophages have been applied in various interdisciplinary research fields such as drug delivery, tissue engineering and biosensor development studies [6]. The most popular application area of filamentous phages is phage display technique where phages expressing a random peptide library on p3 coat proteins are applied in order to identify short specific peptide sequences having binding affinities to other peptides [7], proteins [8], solid materials [9] or cells [10]. For example, Lee et al. constructed bacteriophages which can specifically bind single-walled nanotubes (SWNTs) and $FePO_4$ which were then used to develop high-power lithium ion battery electrodes [11].

Nanodevice fabrication is a fast growing research field employing both bottom-up [12] and top-down [13] manufacturing techniques. Bottom-up fabrication is applied for the production of functional systems via controlled self-assembly of nanoscale building units. There is a tremendous effort to manufacture nanowires (NWs) via bottom-up approach employing self-assembling biotemplates. In nature, there are many examples of self-assembling building blocks. Until now various biomolecules such as DNA [14], viruses [15], microtubules [16], proteins [17] and actin filaments [18] have been applied as building blocks for bottom-up fabrication. Cung et al. have applied bacteriophages as templates for lead zirconate titanate (PZT) NW production [19]. Resulting NWs showed very high piezoelectric constants (132 pm/V). Other than bacteriophages, plant viruses such as tobacco mosaic virus (TMV) molecules have been also investigated for nanobiotechnological applications [20]. Atanasova et al. developed TMV/ZnO hybrid structures to be integrated into field-effect transistors for functional nano-device fabrication [21].

In order to obtain metal decorated biotemplates, either chemical or genetic modifications can be applied. Au–S linkage is one of the most commonly applied technique for obtaining Au–protein hybrid systems. It was previously shown that sulfur carrying amino acids like cysteine have strong binding affinities against Au [22]. Expression of three Met residues on p8 major coat protein subunits of filamentous fd bacteriophages resulted in enhanced Au binding and metallization properties [23]. Slocik et al. applied gold binding peptides (e.g. 12-mer A3 peptide: AYSSGAPPMPPF) identified by phage display technique in order to produce water stabilized AuNPs [24]. They reported that A3 peptides are not only able to bind Au templates but also able to reduce Au ions. The binding of A3 peptide to Au was explained by hydrophobic interactions or hydrogen bonding. After replacing the Tyr residue of A3 peptide with Ser, no reduction occurred showing that the presence of only one Tyr residue enables $HAuCl_4$ reduction. Similarly, Flg tag peptide which also contains one Tyr subunit was reported to be able to reduce Au ions as well. Being inspired by these results, in this study we expressed Tyr containing 5-mer peptides on N-terminal region of major coat protein p8 subunits and compared Au binding affinities and Au reduction potentials of engineered phages. We modified the original N-terminal AEGDD sequence of p8 coat proteins to AYGDD, AYSSG (first five aa of previously identified A3 peptide), YYYYY and tested the Au binding affinities by Quartz crystal microbalance (QCM), Scanning electron microscopy (SEM) and Energy dispersive X-ray spectroscopy (EDX) analyses. One-pot Au metallization reaction was successful without applying additional reducing agents. EDX analyses revealed that recombinant bacteriophages were coated with AuNPs after treatment of phages with different concentrations of AuNPs or with Au clusters after metallization experiments at different $HAuCl_4$ precursor concentrations. Genetically engineered filamentous phages with improved material binding properties may serve as self-assembling nanobiotemplates for bottom-up manufacturing.

2. Materials and methods

2.1. Cloning and phage amplification

Escherichia coli MC1061 (New England Biolabs) and *E. coli* K91BluKan (K91BK-kindly provided by Prof. Dr. Georg P Smith (University of Missouri, USA)) cells were utilized for plasmid and phage amplification correspondingly. Backbone fd-tet vector was delivered by Smith's laboratory. Flexible five aa N-terminal AEGDD region of the major coat protein p8 was substituted with AYGDD, AYSSG (first five aa of previously identified A3 peptide) and YYYYY by assembly polymerase chain reaction (APCR) with the primers listed in Table 1. The first PCR reaction was performed using FP1 & RP1 primers carrying the base pairs coding for desired inserts; and fd-tet vector as the template in order to amplify a 397 bp fragment. Second PCR reaction was conducted in order to amplify a 329 bp fragment having a 5′ overlapping complementary sequence to the first PCR product using primers FP2 & RP2 (Table 1) and the template fd-tet vector. Lastly, the APCR was performed using two PCR products as templates and the far primers FP1 and RP2. Gel extracted and purified APCR product was next treated with restriction enzymes *BsrG*I and *Not*I (NEB) and inserted into the digested fd-tet vector by overnight ligation at 16 °C using T4 DNA ligase (NEB). The ligated vector was transformed into *E. coli* MC1061 cells by electroporation using a micropulser (voltage: 2.5 kV; capacity: 25 μF; resistance: 200 Ω, BIORAD). Transformed cells were plated on Tetracycline (Roth) supplemented LB agar plates for colony selection. Following the sequencing analyses (Eurofins Genomics) *E. coli* K91BK cells were electroporated with vectors of interest and plated on Tetracycline and Kanamycin (Roth) supplemented LB agar plates. Phages were isolated by PEG/NaCl treatment. Purified phages were dialyzed against 1× PBS at 4 °C overnight and stored at 4 °C after quantification by UV–vis spectrometry as previously described [www.biosci.missouri.edu/smithgp/PhageDisplayWebsite/PhageDisplayWebsiteIndex.html].

2.2. Au binding measurements

Au surface binding tests were conducted by QCM measurements with Qsense E1 (Biolin Scientific, Sweden), according to manufacturer's instructions. Gold coated quartz crystals (LOT Quantum Design) were mounted to the instrument's probe arm and 1× PBS was injected to the system until the frequency signal became steady. After 300 μl of bacteriophages (10^{10} cfu/ml in 1× PBS) was given at a flow rate of 15 μl/min, the sensor was washed with autoclaved MilliQ water (18.2 MΩ cm) at the same flow rate. Five overtone resonance frequencies (25, 35, 45, 54 and 64 MHz) were applied for frequency change measurements at 23 °C. Data analysis was performed with QTools software program and experiments were repeated at least for three times.

Affinity of bacteriophages to AuNPs was analyzed by SEM and EDX measurements after incubating the bacteriophages (10^{10} vir/ml) with various dilutions (1:1, 1:3 and 1:10) of 20 nm and 5 nm citrate stabilized AuNPs (Sigma) in 100 μl of 1× PBS. Samples were incubated for 2 h at room temperature on a rolling drum (7 rpm). In order to get more dispersed phage filaments decorated with AuNPs, we decreased the final phage concentrations to 6×10^{10} vir/ml and 6×10^{9} vir/ml (in MilliQ) and conducted the AuNP treatment experiments by mixing 10 μl of phages with 50 μl, 150 μl, 250 μl and 500 μl of 20 nm AuNPs.

2.3. One-pot metallization

One-pot or one-step metallization of phages was performed in 100 mM HEPES buffer (PAN Biotech) without using any additional

Table 1
List of primer sequences used for APCR.

FP1	5′-CTGGTCTGTACACCGTGCAT-3′
RP1_AYGDD	5′-CAGGGAGTCAAAGGCCGCTTTTGCGGGATCGTCACCGTAAGCAGCGAAAGACAGCATC-3′
RP1_AYSSG	5′-CAGGGAGTCAAAGGCCGCTTTTGCGGGACCACTCGAGTAAGCAGCGAAAGACAGCATC-3′
RP1_YYYYY	5′-CAGGGAGTCAAAGGCCGCTTTTGCGGGATAGTAATAGTAGTAAGCGAAAGACAGCATC-3′
FP2	5′-AGCGGCCTTTGACTCCCTG-3′
RP2	5′-TCAACAGTTTCTGCGGCCAGA-3′

reducing agents. Four different experimental conditions were tested at different phage (EXP 1&2: 2×10^{10} vir/ml, EXP 3&4: 10^{11} vir/ml) and $HAuCl_4$ (Sigma) precursor (EXP 1&4: 1 mM, EXP 2&3: 0.6 mM) concentrations. Phages were diluted in 100 mM HEPES buffer at stated concentrations and Au precursor solutions were added finally. After incubation at room temperature for 2 h, samples were prepared for microscopy analyses. In order to prevent excessive aggregation of phages, metallization experiments were next performed under vigorous stirring using magnetic beads on a magnetic stirrer at room temperature for 2 h.

Metallization potential of phages were also tested by QCM analyses. 300 μl of bacteriophages (10^{10} vir/ml in 1× PBS) was injected at a flow rate of 15 μl/min and the Au coated quartz sensor was rinsed with MilliQ at the same flow rate in order to remove unbound phages. Following the washing step, 300 μl of 0.1 mM $HAuCl_4$ or K_2PtCl_4 (Sigma) solutions was injected to the system. 100 mM HEPES buffer was given until the frequency signal was stabilized and the final washing step was performed with MilliQ.

2.4. Microscopy

FEI Quanta 250 FEG scanning electron microscope was used at 30 kV in high vacuum for analyzing the AuNP coated or one-pot metallized phage samples. Elemental analyses were conducted with EDAX™ Team EDX system. Sample preparation was done using industrial scale standard Si wafers with a native oxide layer. SiO_2 wafers were cleaned by sonication for 15 min in 1:1 mixture of acetone and isopropanol. 20 μl of phage solution was dropped on 5 × 5 mm cleaned wafer surface. After 10 min of incubation at 37 °C, excess solution was removed with tissue paper, and 20 μl of sterile MilliQ water was dropped. MilliQ was removed after a few minutes and the samples were blow-dried with nitrogen gas.

Topography measurements were performed at noncontact mode at room temperature and ambient pressure with a Mobile S AFM (Nanosurf AG, Switzerland) having a 110 μm scanning area. Measurements were carried out with Si cantilever tips (Nanoworld AG, Switzerland) at a force constant of 48 N/m and resonance frequency of 190 kHz. Images were analyzed using Gwyddion image processing software (http://gwyddion.net/).

3. Results

3.1. Phage engineering and Au surface binding tests

Sulfur containing amino acids such as Cys and methionine (Met) are widely used for designing peptides with strong metal binding affinities [22]. Lately, we have shown that introducing three Met subunits to N-terminal of major coat protein p8 subunits facilitates MMM-bacteriophage binding to Au surfaces or NPs [23]. Slocik et al. have obtained water stabilized dispersed AuNPs with the help of gold binding peptides identified by phage display technique [24]. It has been reported that A3 peptides (AYSSGAPPMPPF) are not only able to bind Au templates but also able to reduce Au ions [24]. In this study, we tested the effect of Tyr expression on major coat protein p8 subunits on Au binding affinities and Au metallization of recombinant phages. Since five aa of N-terminal of p8 coat protein (AEGDD) are exposed outside, we engineered the wild type AEGDD peptide sequence to AYGDD, AYSSG (first five aa of previously identified A3 peptide) and YYYYY (Fig. 1a). AFM topographic images of engineered bacteriophages demonstrated filamentous phage structures (Fig. 1b). Due to the high concentration of virion particles (10^{11} vir/ml) immobilized on SiO_2 wafer surfaces, phages were observed to form branched filaments. Substitution of Glu (E) residue with one Tyr (Y) enhanced gold binding affinities of engineered AYGDD phages (Fig. 2). Corresponding QCM analyses revealed that although WT fd (AEGDD) phages did not bind on Au coated quartz sensor surfaces, AYGDD phages showed affinity to Au surface with a net frequency decrease of 8.6 ± 4.9 Hz after the final washing step. Additional expression of two Ser (S) residues after the Tyr (Y) provided AYSSG phages with a better Au surface binding affinity with a net frequency decrease of 16.7 ± 5.1 Hz. The strongest binding was observed with YYYYY phages after substituting the five aa of the flexible N-terminal region of p8 coat proteins with five Tyr residues. A net frequency decrease of 25.5 ± 6.5 Hz was recorded for YYYYY phages on Au sensor surfaces.

3.2. AuNP binding analyses of engineered bacteriophages

Engineered bacteriophages were next tested for their AuNP binding affinities. 10^{10} vir/ml of phages were incubated with citrate stabilized 5 nm (Supplementary Data, Fig. 1) and 20 nm AuNPs (Fig. 3) at various dilution factors and analyzed with SEM. Fig. 3 clearly demonstrates that YYYYY phages were decorated with the densest cluster of AuNPs after mixing the phages with 20 nm AuNPs. Presence of Au on phage filaments was confirmed by EDX analyses. C peaks detected on Au coated phages assured the existence of organic material content. When the dilution factor of AuNPs was increased, number of detected AuNPs on phages decreased as predicted (Supplementary Data, Fig. 1). Although YYYYY phages were still observed to be the strongest AuNP binders, WT fd phages did not show any considerable AuNP binding affinity at each dilution factor (Supplementary Data, Fig. 1). In line with Au surface binding experiments conducted by QCM analyses (Fig. 2), AuNP binding tests showed that phages can be listed as YYYYY > AYSSG > AYGDD in terms of their Au binding affinities.

AuNP-phage binding was next investigated at different concentrations of YYYYY phages in order to obtain more defined and less aggregated structures. As 10 μl of 6×10^{10} vir/ml YYYYY phages was mixed with 50 μl of AuNPs, aggregated phage filaments decorated with AuNPs were observed (Fig. 4 – 1st row). As the volume of AuNP solution was increased from 50 μl to 150 μl and 250 μl, denser clusters of AuNPs were detected on phages. In order to see the influence of phage concentration on AuNP binding, ten times less phage (6×10^9 vir/ml) was mixed with the same volumes of AuNP solutions. As the phage concentration was reduced, linearly aligned phage filaments coated with AuNPs were observed where some parts of uncoated bare phage filaments can be recognized as well (Fig. 4 – 2nd row). These results show that the applied phage concentration is critical if we want to obtain well-dispersed phage NWs decorated with AuNPs.

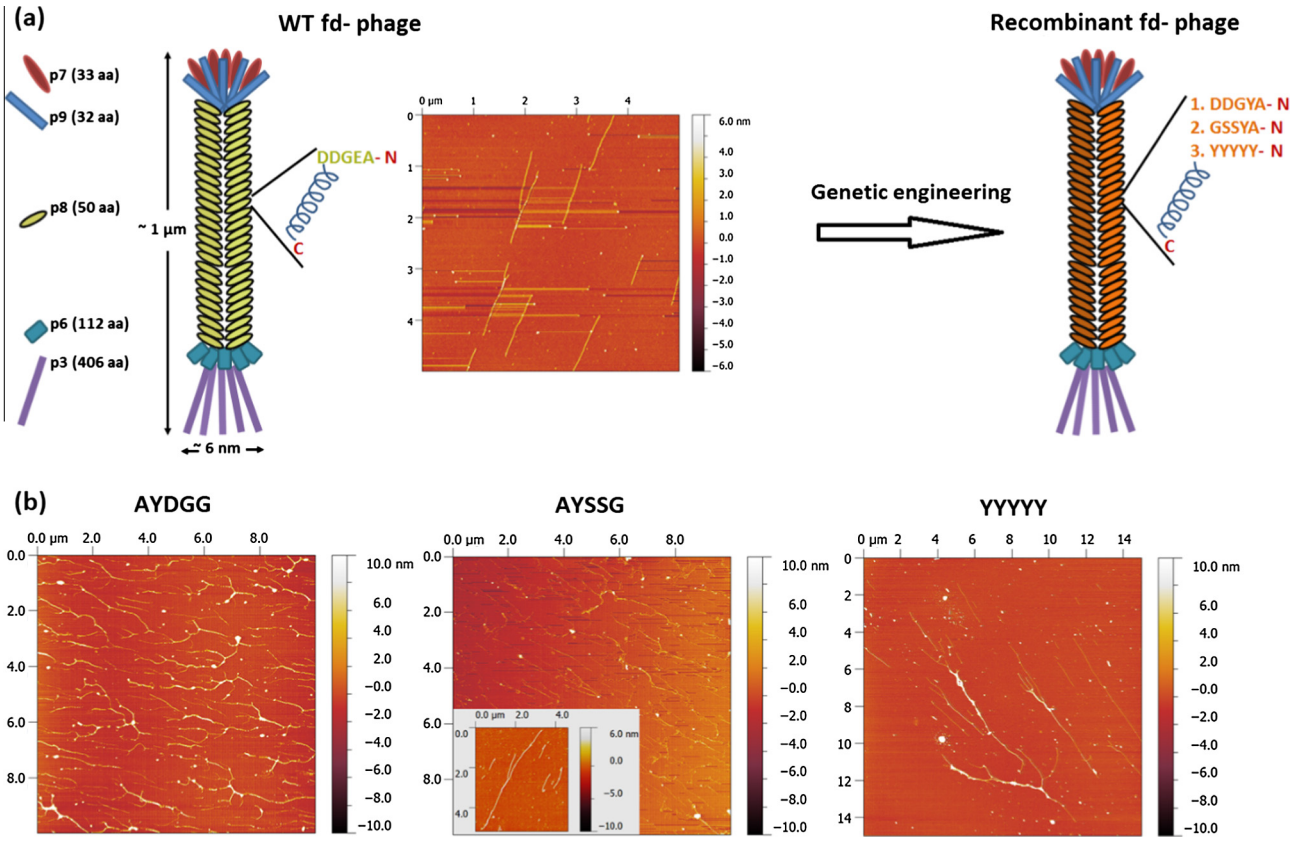

Fig. 1. Schematic representation of WT and genetically engineered fd-phages and the corresponding AFM topography images. (a) WT fd-tet phages are composed of 2700–3000 copies of p8 major coat protein subunits forming a protein cage around 9183 bp circular ssDNA. 5 copies of minor coat proteins p9 and p7 are located on the head part and, p3 and p6 on the tail. Three different phage constructs (AYGDD, AYSSG and YYYYY phages) were obtained by engineering N-terminal five aa overhang region of helical p8 coat proteins. (b) AFM topographic images of engineered AYGDD, AYSSG and YYYYY phages immobilized on SiO_2 wafer surfaces. Measurements were performed in air at ambient conditions.

3.3. One-pot metallization of engineered phages

After demonstrating that YYYYY phages have stronger binding affinities to both Au surfaces and AuNPs by means of QCM and SEM analyses, one-pot metallization potentials of engineered phages were next investigated. It is well known that metal NPs can be deposited on bio-templates like DNA, microtubules, actin filaments or virus particles via chemical reduction reaction. Addition of reducing agents to a mixture of biological molecules and metal precursor solutions results in formation of NPs localized on template surfaces. In this process, metal ions should first bind to active sites of amino acids like histidine, methionine or cysteine present on the template surface, then reducing agents should be added to reduce bound metal ions to metallic atoms and lastly the formation of a critical concentration of metal atoms would result in formation of metal clusters [25]. Here we investigated the one-step metallization of phages in 100 mM HEPES buffer without using any additional reducing agent. Four different experimental conditions were tested at different phage (EXP 1&2: 2×10^{10} vir/ml, EXP 3&4: 10^{11} vir/ml) and $HAuCl_4$ precursor (EXP 1&4: 1 mM, EXP 2&3): 0.6 mM) concentrations. One-step metallization reaction was successful as seen in Fig. 5. For all experimental conditions (Supplementary Data, Fig. 2), extensive metallization was detected for YYYYY phages when compared to AYGDD and WT fd phages. EDX analyses conducted in red boxes confirmed the presence of Au and C peaks detected from metallized Au layers and organic phage materials respectively. AYSSG and YYYYY phages were successfully metallized after EXP 4, although AYGDD and WT fd phages were observed to be partially deposited with Au clusters (Fig. 5). Moreover, SEM images clearly demonstrated larger YYYYY phage aggregates coated with denser Au clusters than AYSSG phages. Therefore, EXP 4 was selected as the optimized one-pot metallization condition for further analyses where 10^{11} vir/ml phages were metallized with 1 mM Au precursor solution.

We next tested the same one-step reaction condition for Pt metallization on Au coated quartz crystal sensor surfaces by QCM analyses. As seen in Fig. 6, after the injection of YYYYY phages and the washing steps, a net frequency decrease of ~25 Hz was recorded showing that the phages bound on Au coated sensors as expected. Subsequent flow of $HAuCl_4$ precursor solution and HEPES buffer resulted in a significant frequency decrease of ~75 Hz after the final washing step showing that the metallization reaction took place (Fig. 6a). On the other hand, a frequency decrease of ~10 Hz was detected for the phages treated with $KPtCl_4$ solution and HEPES buffer after the final washing step implying that the Pt metallization reaction was not as favorable as Au metallization (Fig. 6b). In addition, the experiments conducted in Eppendorf tubes did not reveal any color change for Pt metallization supporting the QCM data (Fig. 6 – inset pictures).

Lastly, we repeated EXP 4 in order to get more segregated smaller filamentous structures instead of larger metallized phage aggregates. We conducted the one-step metallization experiment under vigorous stirring to prevent Au cluster aggregation. As demonstrated in Fig. 7, in line with Fig. 5, WT fd phages did not show a crucial degree of metallization. AYGDD phage filaments were observed to be partially deposited with Au particles. AYSSG and YYYYY phages formed metallized filaments of 1–2 µm long.

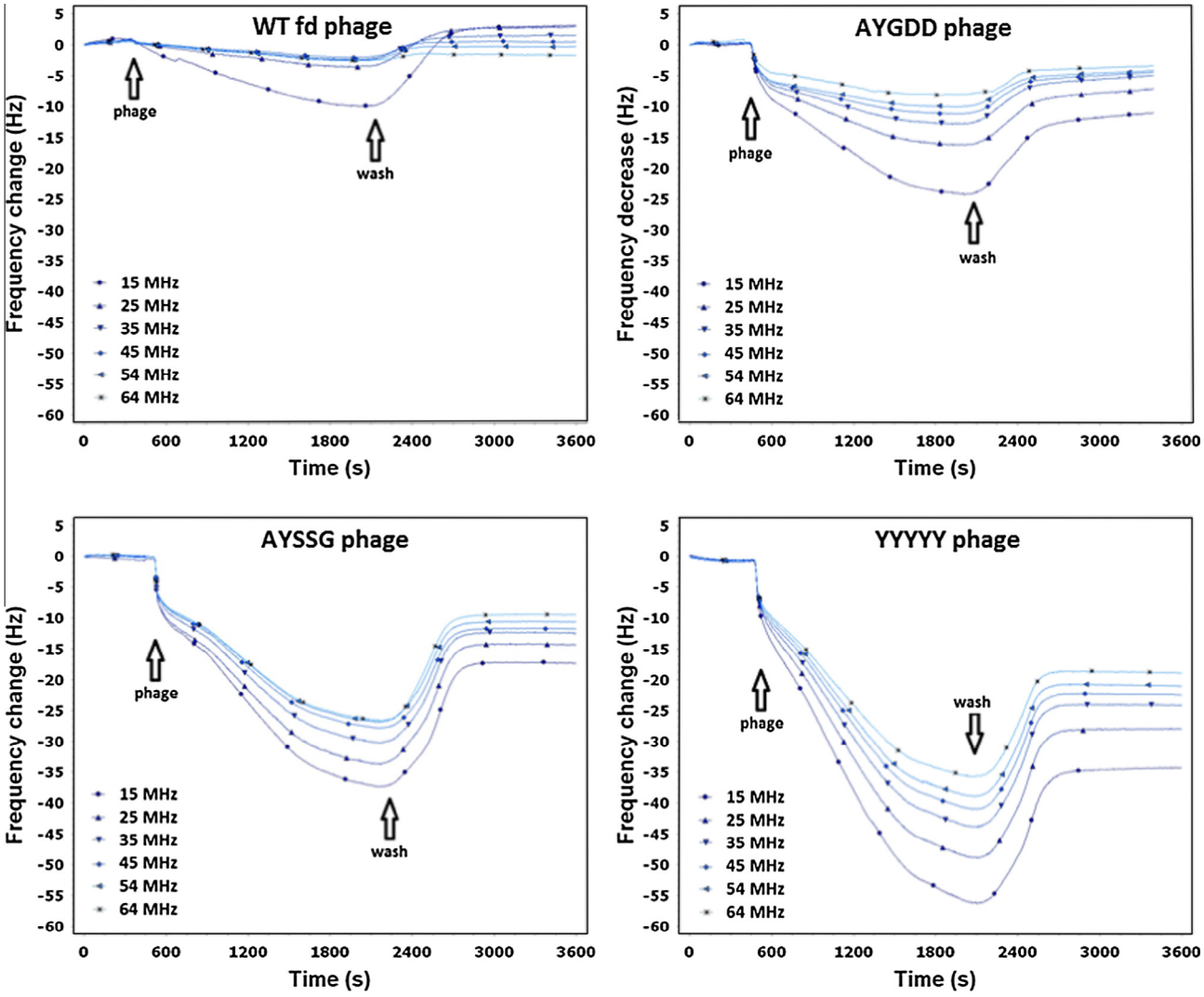

	WT fd	AYGDD	AYSSG	YYYYY
Net resonant frequency decrease (Hz)	-2.3 ± 2.7	8.6 ± 4.9	16.7 ± 5.1	25.5 ± 6.5

Fig. 2. Au surface binding tests of WT and engineered bacteriophages (10^{10} vir/ml) conducted by QCM analyses (operating frequency overtones = 15–64 MHz). WT fd phages showed no specific binding affinity to Au coated quartz crystal sensor surfaces. The strongest affinity to Au surface was recorded for YYYYY phages with a net resonant frequency decrease of 25.5 ± 6.5 Hz followed by AYSSG and AYGDD phages with measured frequency decreases of 16.7 ± 5.1 Hz and 8.6 ± 4.9 Hz respectively. Net frequency changes were calculated at the 3rd frequency overtone ($n = 3$).

YYYYY phages were more densely packed with Au particles than AYSSG phages as expected. The presence of phage organic material was confirmed with C peaks detected by EDX analyses for AYSSG and YYYYY phages. On the other hand, no C peak was detected for (–) control.

4. Discussion

In this study, we investigated the effect of Tyr containing peptide expression on fd phage filaments on Au binding affinities and Au metallization potentials of recombinant phages. In this context, wild type AEGDD peptide sequence, which is the flexible N-terminal region of major coat protein p8, was engineered to AYGDD, AYSSG (first five aa of previously identified A3 peptide) and YYYYY as schematically shown in Fig. 1. QCM analyses revealed that substitution of Glu (E) residue with one Tyr (Y) enhanced gold surface binding affinities of engineered phages (Fig. 2). Expression of two Ser (S) residues after Tyr (Y) increased the Au binding affinities of AYSSG phages further. The strongest binding affinity was achieved with YYYYY phages.

Previously, we have investigated the effect of pH on Au surface binding affinities of fd phages by QCM measurements [23]. No significant phage binding was observed on Au sensors in a broad pH range (pH 3–pH 9). Recently, Mendes et al. have reported on the electron transfer process of hexacyanoferrate (II/III) at Au surfaces

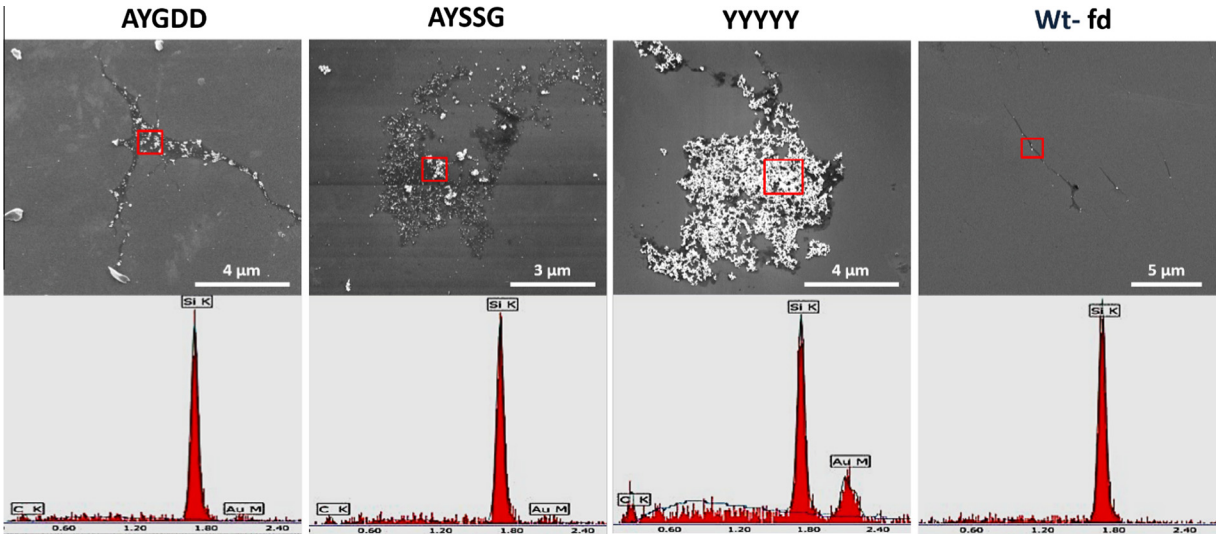

Fig. 3. SEM images of WT and engineered phages (10^{10} vir/ml) incubated with citrate stabilized 20 nm AuNPs. AuNPs were diluted in 100 µl PBS buffer at 1:3 ratio before mixing with the phages. Pictures were taken at 30 kV in high vacuum. EDX analyses were performed inside the red boxes. (For interpretation of the references to color in this figure legend, the reader is referred to the web version of this article.)

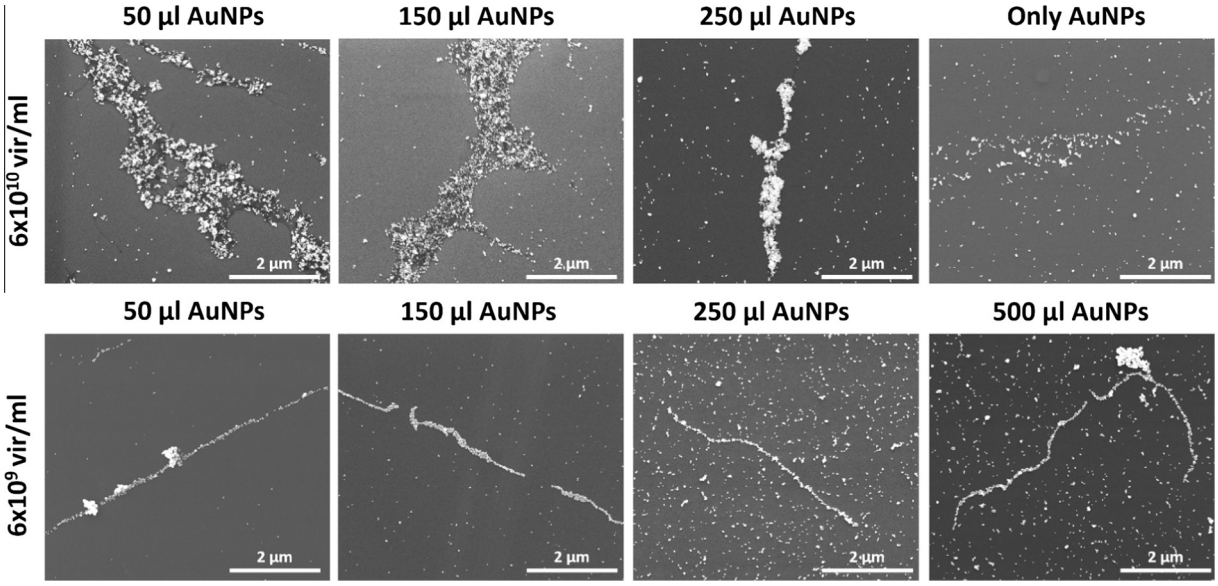

Fig. 4. SEM images of YYYYY phages incubated with citrate stabilized 20 nm AuNPs at various mixing ratios. 10 µl of 6×10^{10} vir/ml or 6×10^{9} vir/ml YYYYY phages were mixed with various volumes of 20 nm AuNPs (50 µl, 150 µl, 250 µl and 500 µl) and investigated with a SEM. Pictures were taken at 30 kV in high vacuum.

functionalized with SAMs [26]. Although SAM coating resulted in different electron transfer responses at different pH values (pH 4–pH 8), bare Au electrodes showed no charge transfer resistance change at various pH values. In line with Mendes et al.'s findings, electrostatic interactions between phage filaments and Au sensor surface can be neglected upon QCM measurements because of the inert nature of Au sensor surface. Moreover, it has been lately reported that it is the chemical nature of amino acid side chains mainly determining the intrinsic affinities of amino acids toward Au surfaces [27]. Thus, Au surface binding of engineered phages detected by QCM analyses in this study can be explained by intrinsic properties of single amino acids expressed on phage filaments.

How single amino acids influence binding affinities of peptides toward Au surfaces is of particular importance. Computational studies were performed in order to investigate the effect of intrinsic properties like hydrophobicity and molecular structure of amino acids on Au binding process. Free energies of interaction (kJ/mol) of 20 amino acids were calculated by Hoefling et al. in order to investigate the binding potentials of single amino acids to Au (1 1 1) surfaces [27]. It has been reported that amino acids with aromatic side chains showed highest absolute values of interaction free energies. For example, Tyr and Trp were noted to have 44.2 and 40.2 kJ/mol of interaction free energies respectively which are considerably higher than Ala (21.9 kJ/mol), Glu (17.5 kJ/mol), Gly (23.6 kJ/mol), Asp (25.5 kJ/mol) forming the wild type flexible N-terminal region of p8 coat protein (AEGDD). Our experimental data are in good agreement with these computational results where we observed stronger Au binding affinities for phage constructs expressing Tyr residues on p8 coat proteins compared to WT phages.

Yu et al. performed a computational study to compare short peptide sequences "AYAS and AYAA" in terms of their Au binding

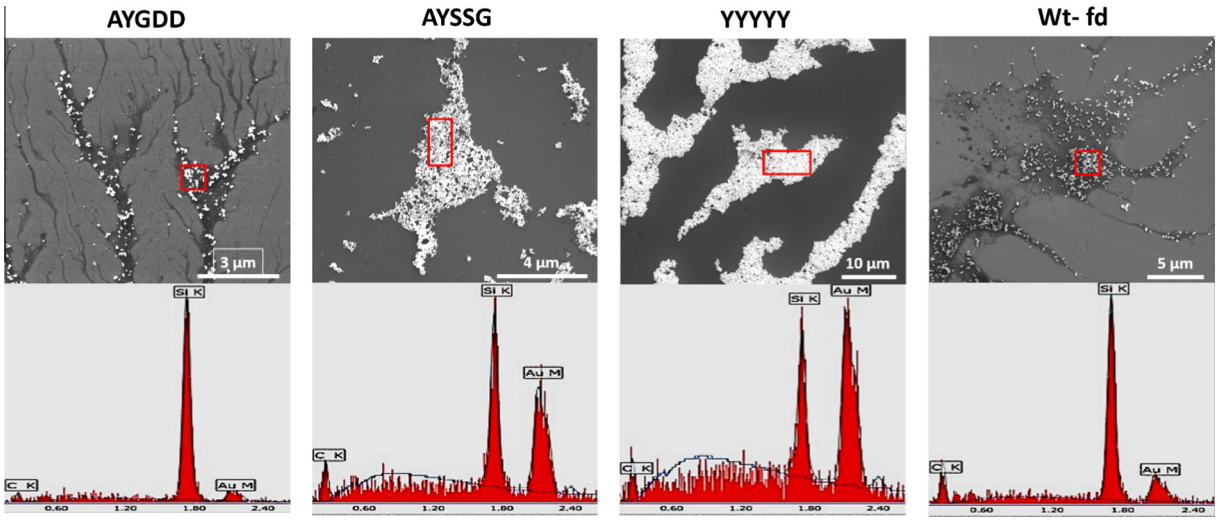

Fig. 5. SEM images of WT and engineered phages after one-pot Au metallization reaction at room temperature for 2 h. Phages were diluted to 10^{11} vir/ml in 100 mM HEPES buffer containing 1 mM $HAuCl_4$ precursor solution (EXP 4). Although AYSSG and YYYYY phages were coated with Au clusters after metallization reaction, AYGDD and WT fd phages were partially deposited with Au particles. EDX analyses conducted in red boxes confirmed the presence of Au and C peaks detected from metallized Au layer and organic phage material respectively. Pictures were taken at 30 kV in high vacuum. (For interpretation of the references to color in this figure legend, the reader is referred to the web version of this article.)

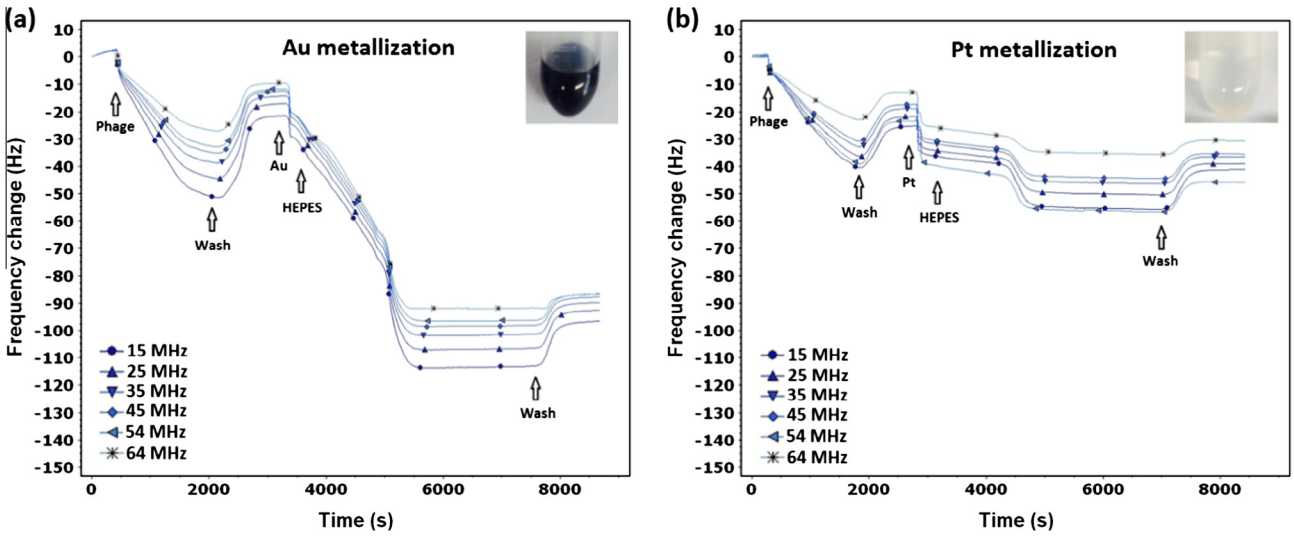

Fig. 6. QCM analyses of recombinant YYYYY phage metallization on Au coated quartz crystal sensor surfaces (operating frequency overtones = 15–64 MHz). YYYYY phages (10^{10} vir/ml in 300 µl 1× PBS) were injected at a flow rate of 15 µl/min. After the washing step, 300 µl of 0.1 mM $HAuCl_4$ or K_2PtCl_4 solutions was given to the system. Significant frequency decrease (~75 Hz at the 3rd overtone) was recorded after 100 mM HEPES buffer injection for $HAuCl_4$ treated phages showing that the metallization reaction took place (a). K_2PtCl_4 treated phages on the other hand demonstrated a frequency decrease of ~10 Hz at the 3rd overtone implying that the metallization reaction for Pt was not as favorable as for Au on YYYYY phages (b). Insets show reaction mixtures after metallization experiments conducted in Eppendorf tubes with 1 mM Au and Pt precursor solutions.

affinities [28]. It has been reported that Tyr and Ser residues are responsible for anchoring and binding to Au surfaces. Due to its less bulky and less hydrophobic side chain, Ser was reported to enable AYAS peptide to anchor faster to Au surfaces. On the other hand, due to their too hydrophobic side groups, Ala residues cannot penetrate into the hydration layer. Therefore, AYAA peptides were shown to anchor to Au surfaces significantly slower than AYAS peptides. Since the only difference between two peptides is Ser residue, Yu et al., have concluded that Ser is mainly responsible for the peptide anchoring [28]. In this study, QCM analyses showed that when Gly3 and Glu4 residues were replaced by two Ser units, an increase in frequency change was detected on Au sensor chip surface showing that Au binding affinity of AYSSG phages was stronger than AYGDD phages (Fig. 2) most probably due to the enhanced Au surface anchoring properties caused by expressed Ser residues. Tomczak et al. modified the A3 peptide as such that Ser3 and Ser4 residues were substituted with Pro residues (A3-P) [29]. Almost no AuNP binding was observed after removing the Ser subunits from A3 peptide showing that hydroxyl group containing Ser amino acids provide strong Au binding. Our AuNP binding tests support these findings as we showed that AYGDD phages bind less NPs than AYSSG phages (Supplementary Data, Fig. 1). In addition, it was reported by Braun et al. that peptides carrying Ser and Tyr demonstrated stronger Au binding properties [30]. Computer simulation studies showed that A3-P peptide could not anchor to the Au surface due to the rigid ring structure of Pro residues making the peptide backbone unflexible for binding [28]. Due to bulkier rigid ring structures, A3-P peptides were unsuccessful in

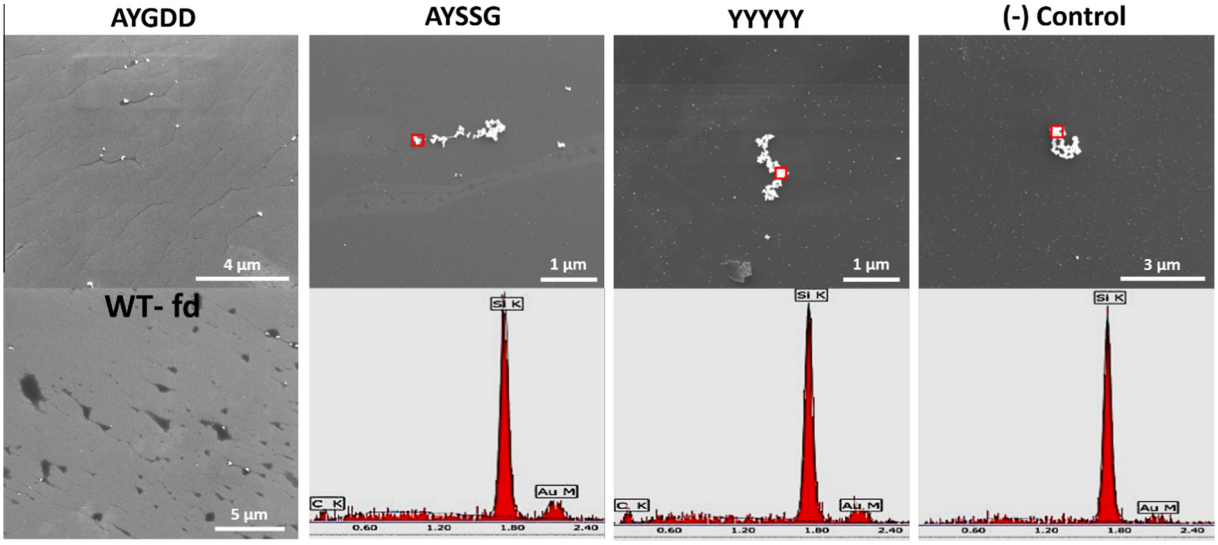

Fig. 7. SEM images of engineered and WT phages (10^{11} vir/ml) metallized using 1 mM $HAuCl_4$ and 100 mM HEPES buffer solution after one-step metallization reaction (EXP 4). Reaction was conducted under vigorous stirring in order to prevent Au cluster aggregation. Pictures were taken at 30 kV in high vacuum. EDX analyses were performed inside the red boxes. (For interpretation of the references to color in this figure legend, the reader is referred to the web version of this article.)

penetrating into the hydration layer hindering Au surface binding. Backbone flexibility is one of the most important properties for peptides to anchor and bind on surfaces provided by amino acids like Gly and Ala. These amino acids do not possess any bulky side groups which may negatively affect the peptide's conformation [28]. Thus, Ala and Gly residues stabilize the structural conformation of AYSSG peptides by providing backbone flexibility.

Yu et al. have investigated the distance between the Au surface and heavy atoms of A3 peptide in order to study the equilibrium configuration [28]. It was seen that Met, Tyr and Phe residues were able to bind on Au surface via sulfur containing functional groups or aromatic side chains providing stronger binding energies. Simulation studies have confirmed the strong binding of aromatic side chains of Tyr and Phe to Au (1 1 1) surface. It has been reported that molecular structures of the aromatic rings of Tyr and Phe fit the Au (1 1 1) surface structure providing tighter binding in line with other simulation studies on binding energies of amino acids [28,31]. In line with these observations, in our study, AYGDD phages were observed to bind on Au sensor surfaces stronger than AEGDD (WT fd) phages due to the presence of one Tyr residue (Fig. 2). Moreover, after Glu2 of wild type AEGDD phages was substituted with a Tyr residue, AYGDD phages were observed to have stronger binding affinities to AuNPs than AEGDD phages (Fig. 3). Finally, the expression of five Tyr residues on p8 coat protein increased AuNP binding affinities of phages considerably making YYYYY phages the strongest AuNP binders implying that Tyr plays a very important role in AuNP binding mechanism. In addition to intrinsic binding affinity of Tyr toward Au which was confirmed by computational studies by calculating interaction free energies, electrostatic properties of phage filaments may play an important role on binding of engineered phages to AuNPs in buffer solution. Theoretical isoelectric points (pIs) of mature p8 coat proteins (50 aa) carrying N-terminal YYYYY, AYSSG, AYGDD and AEGDD peptides were calculated as 9.31, 9.53, 8.31 and 6.28 respectively. Citrate stabilized AuNPs were previously reported to be negatively charged in a broad pH range (pH 3–pH 8) [32]. At pH 7 where AuNP binding experiments were conducted, although WT AEGDD phages were negatively charged; AYGDD, AYSSG and YYYYY phage surfaces were positively charged inducing attractive electrostatic forces between engineered phages and negatively charged AuNPs. Supportingly, AuNP binding tests showed that although WT phages did not have a significant binding affinity to AuNPs, engineered phages attracted considerably more AuNPs (AYGDD < AYSSG < YYYYY) (Fig. 3). Whilst the pIs of AYSSG and YYYYY are similar, we observed more AuNP binding for YYYYY phages implying the existence of a combined effect of electrostatic and intrinsic molecular interactions between the displayed amino acids and the Au surface.

Tyr and Trp were reported to be able to reduce chloroaurate ions [33,34]. According to Yu et al.'s theoretical calculations, Cl^- ions can be replaced from chloroaurate ions by Tyr and Ser residues [28]. Due to the increase in electron affinities of Tyr and Ser residues after gold binding, Au (III) reduction can easily occur. Computational studies have shown that Tyr has higher Au (III) reduction potential than Ser which has also been demonstrated experimentally by replacing Tyr2 of A3 peptide with Ser residue resulting in less gold binding affinity [29]. Similarly, SEM analyses revealed that denser Au clusters were deposited on YYYYY phages than AYSSG phages after the one-step metallization reaction (Fig. 5) showing the impact of Tyr residues on metallization potential of engineered phages.

HEPES buffer (p*Ka* = 7.6) is commonly applied in biology as one of "Good's Buffers" with hydrogen ion buffering characteristic and low binding affinities to transition metals [35]. Stanley et al. published on reducing activity of HEPES buffer on $HAuCl_4$ precursor solution [35]. In this study, reduction specificity of HEPES against Au was tested by performing the same reaction with Pt precursor solution. We did not observe any Pt metallization (Fig. 6) implying that HEPES buffer is especially acting on $HAuCl_4$. It has been previously demonstrated that nitrogen-centered cationic free radicals can be exposed by HEPES buffer in the presence of Au (III) ions, forming AuNPs without any need of reducing agents [36]. Similarly, we observed Au cluster formation for our control samples as well without any phages (Fig. 7). For the samples containing phages, on the other hand, we observed different metallization potentials in terms of Au cluster coverage on phage filaments as demonstrated by SEM and EDX analyses (Figs. 5 and 7) implying that the metallization reaction was phage mediated. In addition to HEPES buffer's reducing activity, Tyr and Ser residues were previously reported to reduce Au (III) [28,29]. Thus, in our one-pot metallization system, it is reasonable to have reduction activities from both HEPES buffer and from displayed amino acids at the

same time. In order to show the effect of displayed peptides on Au reduction potentials of engineered phages, we performed one-pot metallization reaction in PBS buffer instead of HEPES buffer (Supplementary Data, Fig. 3). For control samples without any phages, no significant reduction was seen. Only a few particles were visible on SEM images. YYYYY phages were observed to be decorated with more reduced particles compared to AYSSG and AYGDD phages. Moreover, AYSSG phages induced more Au reduction than AYGDD phages most probably due to the existence of additional Ser residues which were previously shown to be able to reduce Au (III) [28,29]. WT fd phages, on the other hand, were observed to be coated with a few particles. Although we observed some reduced particles on phage filaments for reduction experiments conducted in PBS, we could not see a macroscopic color change in Eppendorf tubes after the reaction in contrast to HEPES buffer. This implies that HEPES buffer increases the reduction potential of Au (III) by engineered phages significantly. Thus the reduction reaction in HEPES buffer should be a combined effect of reducing activities of amino acids and the buffer itself. Cl^- ions can be replaced from chloroaurate ions by Tyr and Ser residues according to Yu et al.'s computational calculations [28]. Thus, Au (III) reduction can readily occur due to the increased electron affinities of Tyr and Ser residues after gold binding. In line with Yu et al.'s report, in our experiments, Tyr and Ser residues displayed on bacteriophage filaments most probably followed a similar reduction pathway. As soon as the first Au (0) atoms were formed on phages, they acted as nucleation points for further Au cluster growth due to the combined reducing activities of HEPES buffer and Tyr-Ser residues. Finally, we obtained phage filaments decorated with Au particles as shown by SEM and EDX analyses (Figs. 5 and 7).

5. Conclusions

In this study, we constructed genetically engineered bacteriophages by expressing Tyr containing 5-mer peptides on N-terminal region of major coat protein p8 subunits and compared their Au binding affinities and Au reduction potentials. N-terminal AEGDD sequence of p8 coat proteins were modified to AYGDD, AYSSG and YYYYY sequences. QCM, SEM and EDX analyses were applied for Au affinity tests. QCM analyses revealed that substitution of Glu (E) residue with one Tyr (Y) enhanced the gold surface binding affinities of engineered phages. By substituting the five aa of the flexible N-terminal region of p8 coat proteins with five Tyr residues, the strongest Au binding affinity was achieved with YYYYY phages. Similarly, SEM analyses demonstrated that AYGDD phages showed stronger binding affinities to AuNPs than AEGDD phages. Expression of five Tyr residues on p8 coat protein subunits further increased AuNP binding affinities of engineered phages making YYYYY phages the strongest AuNP binders showing that Tyr plays a very important role in AuNP binding mechanism. One-step Au metallization reaction was successful without applying any additional reducing agent. SEM and EDX analyses revealed the presence of either AuNPs or Au clusters deposited on phage filaments after incubating the phages with different concentrations of AuNPs or after one-pot metallization experiments conducted at different phage and $HAuCl_4$ precursor concentrations. SEM analyses showed the existence of denser Au clusters deposited on YYYYY phages than AYSSG phages after one-step metallization revealing the importance of Tyr residues on metallization potential of engineered phages. Moreover, expression of two Ser residues instead of two Gly units following the Tyr residue increased the Au metallization potential of AYSSG phages over AYGGD phages showing the effect of Ser units on Au reduction and binding process. Such genetically engineered filamentous phages with improved material binding properties may serve as self-assembling nanobiotemplates for bottom-up manufacturing.

Acknowledgment

This work was financed by Korea Institute of Science and Technology – Europe basic research program.

Appendix A. Supplementary material

Supplementary data associated with this article can be found, in the online version, at http://dx.doi.org/10.1016/j.jcis.2015.05.006.

References

[1] D.A. Marvin, L.C. Welsh, M.F. Symmons, W.R.P. Scott, S.K. Straus, J. Mol. Biol. 355 (2006) 294–309.
[2] J. Lubkowski, F. Hennecke, A. Plückthun, A. Wlodawer, Structure 7 (1999) 711–722.
[3] Y.A. Wang, X. Yu, S. Overman, M. Tsuboi, G.J. Thomas Jr, E.H. Egelman, J. Mol. Biol. 361 (2006) 209–215.
[4] D.A. Marvin, Curr. Opin. Struct. Biol. 8 (1998) 150–158.
[5] S.K. Straus, W.R.P. Scott, M.F. Symmons, D.A. Marvin, Eur. Biophys. J. 37 (2008) 521–527.
[6] M. Henry, L. Debarbieux, Virology 434 (2012) 151–161.
[7] Z. Zhang, W. Zhu, T. Kodadek, Nat. Biotechnol. 18 (2000) 71–74.
[8] I. López, M.A. Pardo, J. Immunol. Methods 373 (2011) 247–251.
[9] S.R. Whaley, D.S. English, E.L. Hu, P.F. Barbara, A.M. Belcher, Nature 405 (2000) 665–668.
[10] M. Whitney, J.L. Crisp, E.S. Olson, T.A. Aguilera, L.A. Gross, L.G. Ellies, R.Y. Tsien, J. Biol. Chem. 285 (2010) 22532–22541.
[11] Y.J. Lee, H. Yi, W.J. Kim, K. Kang, D.S. Yun, M.S. Strano, G. Ceder, A.M. Belcher, Science 324 (2009) 1051–1055.
[12] Y. Huang, C.Y. Chiang, S.K. Lee, Y. Gao, E.L. Hu, J.D. Yoreo, A.M. Belcher, Nano Lett. 5 (2005) 1429–1434.
[13] Y. Yan, Z. Hu, X. Zhao, T. Sun, S. Dong, X. Li, Small 6 (2010) 724–728.
[14] C. Erler, K. Günther, M. Mertig, Appl. Surf. Sci. 255 (2009) 9647–9651.
[15] E. Dujardin, C. Peet, G. Stubbs, J.N. Culver, S. Mann, Nano Lett. 3 (2003) 413–417.
[16] J.C. Zhou, X. Wang, M. Xue, Z. Xu, T. Hamasaki, Y. Yang, K. Wang, B. Dunn, Mater. Sci. Eng., C 30 (2010) 20–26.
[17] N. Korkmaz, F. Börrnert, D. Köhler, R.G. Mendes, A. Bachmatiuk, M.H. Rümmeli, B. Büchner, L.M. Eng, G. Rödel, Nanotechnology 22 (2011) 375606.
[18] F. Patolsky, Y. Weizmann, I. Willner, Nat. Mater. 3 (2004) 692–695.
[19] K. Cung, B.J. Han, T.D. Nguyen, S. Mao, Y.W. Yeh, S. Xu, R.R. Naik, G. Poirier, N. Yao, P.K. Purohit, M.C. McAlpine, Nano Lett. 13 (2013) 6197–6202.
[20] M. Young, D. Willits, M. Uchida, T. Douglas, Annu. Rev. Phytopathol. 46 (2008) 361–384.
[21] P. Atanasova, D. Rothenstein, J.J. Schneider, R.C. Hoffmann, S. Dilfer, S. Eiben, C. Wege, H. Jeske, J. Bill, Adv. Mater. 23 (2011) 4918–4922.
[22] M. Honda, Y. Baba, N. Hirao, T. Sekiguchi, J. Phys: Conf. Ser. (2008), http://dx.doi.org/10.1088/1742-6596/100/5/052071.
[23] N. Korkmaz, Colloids Surf. B Biointerfaces 112C (2013) 219–228.
[24] J.M. Slocik, M.O. Stone, R.R. Naik, Small 1 (2005) 1048–1052.
[25] Y. Yang, B.H. Constance, P.A. Deymier, J. Hoying, S. Raghavan, J.J. Zelinski, J. Mater. Sci. 39 (2004) 1927–1933.
[26] R.K. Mendes, R.S. Freire, C.P. Fonseca, S. Neves, L.T. Kubota, J. Braz. Chem. Soc. 15 (2004) 849–855.
[27] M. Hoefling, F. Iori, S. Corni, K.E. Gottschalk, Langmuir 26 (2010) 8347–8351.
[28] J. Yu, M.L. Becker, G.A. Carri, Langmuir 28 (2011) 1408–1417.
[29] M.M. Tomczak, J.M. Slocik, M.O. Stone, R.R. Naik, Biochem. Soc. Trans. 35 (2007) 512–515.
[30] R. Braun, M. Sarikaya, K. Schulten, J. Biomater. Sci. Polym. Ed. 13 (2002) 747–757.
[31] H. Heinz, B.L. Farmer, R.B. Pandey, J.M. Slocik, S.S. Patnaik, R. Pachter, R.R. Naik, J. Am. Chem. Soc. 131 (2009) 9704–9714.
[32] A.A. Khan, E.K. Fox, M.Ł. Górzny, E. Nikulina, D.F. Brougham, C. Wege, A.M. Bittner, Langmuir 29 (2013) 2094–2098.
[33] J.M. Slocik, R.R. Naik, M.O. Stone, D.W. Wright, J. Mater. Chem. 7 (2005) 749–753.
[34] S. Si, T.K. Mandal, Chemistry 13 (2007) 3160–3168.
[35] S.K. Stanley, M.L. Becker, E.K. Lin, W.L. Wu, Langmuir 25 (2009) 10886–10892.
[36] R. Chen, J. Wu, H. Li, G. Cheng, Z. Lu, C.M. Che, Rare Met. 29 (2010) 180–186.